Inorg. Chem. **2004**, *43*, 1857−1864

2D−3D Transformation of Layered Perovskites through Metathesis: Synthesis of New Quadruple Perovskites $A_2La_2CuTi_3O_{12}$ (A = Sr, Ca)

T. Sivakumar,[†] K. Ramesha,[‡] S. E. Lofland,[§] K. V. Ramanujachary,[§] G. N. Subbanna,[†] and J. Gopalakrishnan*,[†]

Solid State and Structural Chemistry Unit, Materials Research Centre, Indian Institute of Science, Bangalore-560 012, India, Materials Department, University of California, Santa Barbara, California 93106, and Department of Chemistry and Biochemistry, Rowan University, Glassboro, New Jersey 08028

Received November 24, 2003

We describe the synthesis of two new quadruple perovskites, $Sr_2La_2CuTi_3O_{12}$ (**I**) and $Ca_2La_2CuTi_3O_{12}$ (**II**), by solid-state metathesis reaction between $K_2La_2Ti_3O_{10}$ and $A_2CuO_2Cl_2$ (A = Sr, Ca). **I** is formed at 920 °C/12 h, and **II**, at 750 °C/24 h. Both the oxides crystallize in a tetragonal (*P*4/*mmm*) quadruple perovskite structure (a = 3.9098(2) and c = 15.794(1) Å for **I**; a = 3.8729(5) and c = 15.689(2) Å for **II**). We have determined the structures of **I** and **II** by Rietveld refinement of powder XRD data. The structure consists of perovskite-like octahedral $CuO_{4/2}O_{2/2}$ sheets alternating with triple octahedral $Ti_3O_{18/2}$ sheets along the *c*-direction. The refinement shows La/A disorder but no Cu/Ti disorder in the structure. The new cuprates show low magnetization (0.0065 μ_B for **I** and 0.0033 μ_B for **II**) suggesting that the Cu(II) spins are in an antiferromagnetically ordered state. Both **I** and **II** transform at high temperatures to 3D perovskites where La/Sr and Cu/Ti are disordered, suggesting that **I** and **II** are metastable phases having been formed in the low-temperature metathesis reaction. Interestingly, the reaction between $K_2La_2Ti_3O_{10}$ and $Ca_2CuO_2Cl_2$ follows a different route at 650 °C, $K_2La_2Ti_3O_{10} + Ca_2CuO_2Cl_2 \rightarrow CaLa_2Ti_3O_{10} + CaCuO_2 + 2KCl$, revealing multiple reaction pathways for metathesis reactions.

Introduction

We have described previously[1,2] transformations of layered perovskites of both Ruddlesden−Popper (R−P) and Dion−Jacobson (D−J) series to new layered perovskites by metathesis reactions. For example, the reaction of $K_2La_2Ti_3O_{10}$ (n = 3, R−P phase) with BiOCl yields the Aurivillius (A) phase[1] $(Bi_2O_2)La_2Ti_3O_{10}$, while the reaction of $NaLaTiO_4$ (n = 1, R−P phase) with BiOCl yields $(BiO)LaTiO_4$, a novel R−P/A hybrid phase.[2] Other transformations of layered perovskite oxides have also been reported in the literature. Sugimoto et al.[3] have transformed the A phase, $Bi_2O_2(SrNaNb_3O_{10})$, to the R−P phase, $H_2SrNaNb_3O_{10}$, by acid-leaching, which selectively removes the interlayer Bi_2O_2 sheets. Similarly, Schaak and Mallouk[4] have transformed layered $K_2Eu_2Ti_3O_{10}$ (R−P phase) to the three-dimensional (3D) perovskite, $A^{II}Eu_2Ti_3O_9$, by 2 K^+/A^{2+} (A = Ca, Sr) ion exchange, followed by Eu^{III}/Eu^{II} reduction in hydrogen. These developments in the design of perovskite oxides through new soft chemical reactions have been reviewed by Schaak and Mallouk.[5]

Continuing our efforts to synthesize new perovskite related oxides through metathesis, we focused on oxides-containing CuO_2 sheets, in view of the importance of such oxides toward superconductivity.[6] $Sr_2CuO_2Cl_2$ and $Ca_2CuO_2Cl_2$ are two well-known layered perovskite oxide chlorides,[7] possessing $K_2NiF_4 \equiv La_2CuO_4$ related structures (Figure 1), where the

* To whom correspondence should be addressed. E-mail: gopal@sscu.iisc.ernet.in.
[†] Indian Institute of Science.
[‡] University of California.
[§] Rowan University.

(1) Gopalakrishnan, J.; Sivakumar, T.; Ramesha, K.; Thangadurai, V.; Subbanna, G. N. *J. Am. Chem. Soc.* **2000**, *122*, 6237−6241.
(2) Sivakumar T.; Seshadri, R.; Gopalakrishnan, J. *J. Am. Chem. Soc.* **2001**, *123*, 11496−11497.
(3) Sugimoto, W.; Shirata, M.; Sugahara, Y.; Kuroda, K. *J. Am. Chem. Soc.* **1999**, *121*, 11601−11602.
(4) Schaak, R. E.; Mallouk, T. E. *J. Am. Chem. Soc.* **2000**, *122*, 2798−2803.
(5) Schaak, R. E.; Mallouk, T. E. *Chem. Mater.* **2002**, *14*, 1455−1471.
(6) (a) Sleight, A. W. *Science* **1988**, *242*, 1519−1527. (b) Cava, R. J. *J. Am. Ceram. Soc.* **2000**, *83*, 5−28.
(7) (a) Grande, V. B.; Müller-Buschbaum, Hk. *Z. Anorg. Allg. Chem.* **1975**, *417*, 68−74. (b) Grande, V. B.; Müller-Buschbaum, Hk. *Z. Anorg. Allg. Chem.* **1977**, *429*, 88−90.

10.1021/ic035358l CCC: $27.50
Published on Web 02/13/2004

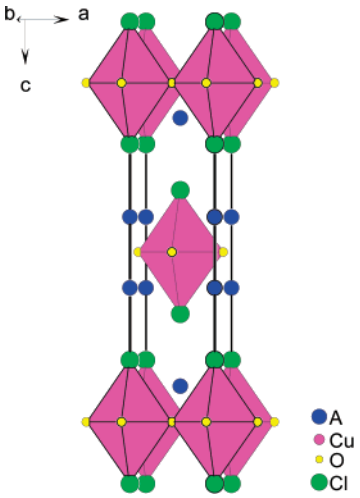

Figure 1. Structure of $A_2CuO_2Cl_2$ (A = Sr, Ca).

chlorine atoms occupy the apical positions of $CuO_{4/2}Cl_2$ octahedra. Considering the dimensional compatibility of $A_2CuO_2Cl_2$ (A = Sr, Ca) and the R−P phases such as $K_2La_2Ti_3O_{10}$ in the *a*−*b* plane, we believed that a metathesis reaction of the type

$$K_2La_2Ti_3O_{10} + A_2CuO_2Cl_2 \rightarrow A_2La_2CuTi_3O_{12} + 2KCl \quad (1)$$

would occur in the solid state at relatively low temperatures, yielding novel quadruple perovskite oxides, $A_2La_2CuTi_3O_{12}$ (A = Sr, Ca), where $[ACuO_2]^{2+}$ and $[La_2Ti_3O_{10}]^{2-}$ slabs would stack alternately along the *c*-axis. Our investigations show that the metathesis (eq 1) indeed occurs at 750−920 °C yielding new quadruple perovskite oxides, as expected. The details of synthesis and structural characterization together with electrical and magnetic properties of the new phases are described in this paper.

Experimental Section

Synthesis. $K_2La_2Ti_3O_{10}$ was prepared by reacting stoichiometric quantities of KNO_3, La_2O_3 (predried at 900 °C), and TiO_2 at 1000 °C in air for 48 h with one intermediate grinding. Excess KNO_3 (25 mol %) was added to compensate for the loss due to volatilization. $Sr_2CuO_2Cl_2$ was prepared[7a] by reacting stoichiometric quantities of $SrCl_2$, $SrCO_3$, and CuO at 800 °C in N_2 for 18 h with one intermediate grinding. $Ca_2CuO_2Cl_2$ was obtained by mixing stoichiometric quantities of CaO and $CuCl_2 \cdot 2H_2O$ in *n*-hexane; the reactants were heated in air at 200 °C for 3 h, and then the temperature was slowly (2 °C/min) raised to 750 °C and kept at this temperature for 9 h.

Reaction between $K_2La_2Ti_3O_{10}$ and $Sr_2CuO_2Cl_2$ in the solid state was investigated by heating a stoichiometric mixture of the reactants at various temperatures and duration in air. Examination of the products by powder X-ray diffraction (XRD) revealed that the reaction occurred according to eq 1 at 920 °C in air, yielding a novel layered perovskite $Sr_2La_2CuTi_3O_{12}$ (**I**) and KCl as products. The product was washed with distilled water to remove KCl and dried at 110 °C. Similarly, the reaction between $K_2La_2Ti_3O_{10}$ and $Ca_2CuO_2Cl_2$ was found to yield a new layered perovskite, $Ca_2La_2CuTi_3O_{12}$ (**II**) at 750 °C. Both **I** and **II** were found to transform to simple cubic perovskite/double perovskite structures at higher temperatures (1000−1100 °C).

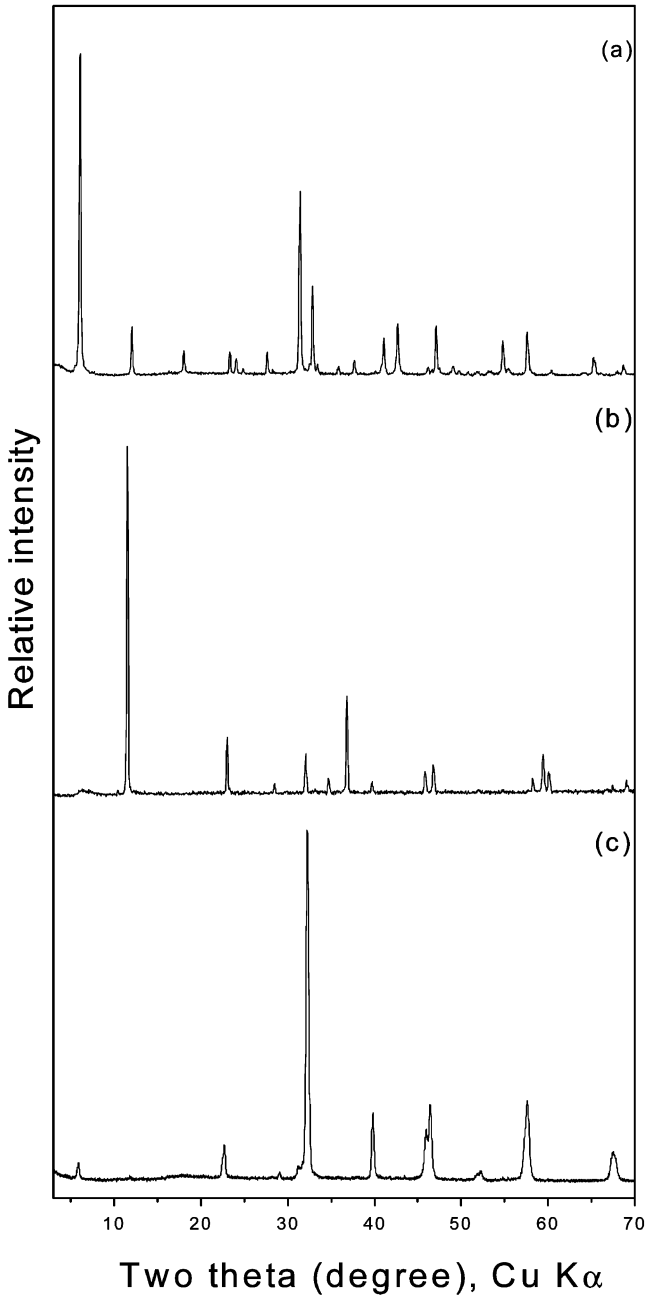

Figure 2. Powder XRD patterns of (a) $K_2La_2Ti_3O_{10}$, (b) $Sr_2CuO_2Cl_2$, and (c) $Sr_2La_2CuTi_3O_{12}$ (**I**).

Characterization. The products were characterized at various stages of the reaction by powder XRD (Siemens D-5005 powder diffractometer, Cu Kα radiation). Unit cell parameters of single-phase materials were determined by least-squares refinement of the powder XRD data using the PROSZKI[8] program. Structural refinements of the powder XRD data were carried out by the Rietveld method using the XND program.[9] For structure refinement, the data were collected in the 2θ range 3−100° with a step size of 0.02° and a step time of 7 s. Single-phase products were also

(8) Losocha, W.; Lewinski, K. *J. Appl. Crystallogr.* **1994**, *27*, 437−438.
(9) Bérar, J.-F. *Program XND*; ESRF: Grenoble, France. More information under: http://www.ccp14.ac.uk. Bérar, J.-F. *Proceedings of the IUCr satellite Meeting on Powder Diffractometry*, Toulouse, France, July 1990. Bérar J.-F.; Garnier, P. *II APD Conference*; NIST: Gaithersburg, MD, May 1992. Bérar J.-F.; Garnier, P. *NIST Spec. Publ.* **1992**, *846*, 212.

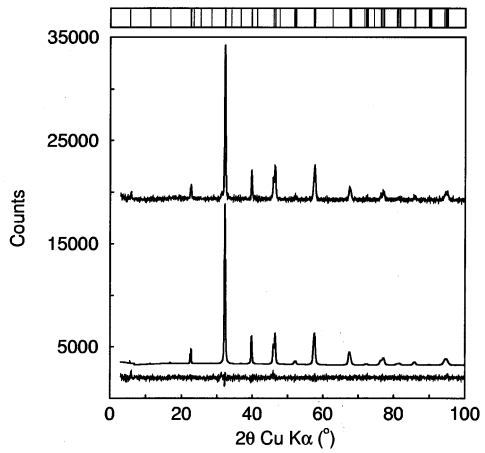

Figure 3. Observed (top), Rietveld refined (middle), and difference (bottom) XRD profiles of $Sr_2La_2CuTi_3O_{12}$. Vertical lines on the top panel above the figure indicate the expected Bragg reflections in the space group *P*4/*mmm*.

characterized by scanning electron microscopy (SEM) and elemental analyses by energy-dispersive X-ray spectroscopy (EDX) (JEOL-JSM-5600 LV scanning electron microscope at a 20 kV accelerating voltage fitted with an Oxford Instruments Be window detector). Electron diffraction (ED) patterns were recorded using a JEOL JEM 200-CX transmission electron microscope. Dc magnetization measurements were performed with a Physical Property Measuring System (PPMS) of Quantum Design Inc., San Diego, California (U.S.) featuring a 9 T magnet. Magnetization was measured at constant field values as the temperature was varied between 5 and 300 K. The field ranged from 0.5 to 5 T. At 5 K, the magnetization at various fields was plotted and extrapolated from high field to zero. The intercept was taken as the net moment. Dc electrical resistivity measurements were carried out on sintered pellets by a four-probe technique using a closed-cycle helium cryostat that goes down to 15 K.

Results and Discussion

We followed the solid-state reaction between $K_2La_2Ti_3O_{10}$ and $Sr_2CuO_2Cl_2$ by heating a stoichiometric mixture of the reactants at various temperatures and duration in air. Examination of the products by powder XRD showed that the reaction occurred around 900 °C yielding a new phase. The reaction was complete at 920 °C after 12 h. Reflections due to starting materials were completely absent. New reflections together with KCl reflections were seen in the product, suggesting that the reaction between $K_2La_2Ti_3O_{10}$ and $Sr_2CuO_2Cl_2$ followed the metathesis pathway (eq 1). The XRD pattern of the product (**I**) (Figure 2), after washing with distilled water and drying at 110 °C in an air oven, could be indexed on a tetragonal system with $a = 3.905(1)$ and $c = 15.78(3)$ Å. SEM and EDX analysis showed that product **I** was a single phase with Sr:La:Cu:Ti ratio of 2:2:1:3 (within ±0.05) as expected for the formula $Sr_2La_2CuTi_3O_{12}$. Also, no chloride was detected in the EDX spectrum indicating complete transformation of the starting materials.

We have determined the structure of $Sr_2La_2CuTi_3O_{12}$ (**I**) by Rietveld refinement of powder XRD data. Observed, calculated, and difference profiles for **I** are shown in Figure 3. The atomic positions and bond lengths are listed in Tables 1 and 2, respectively. In Figure 4a, we show the structure of

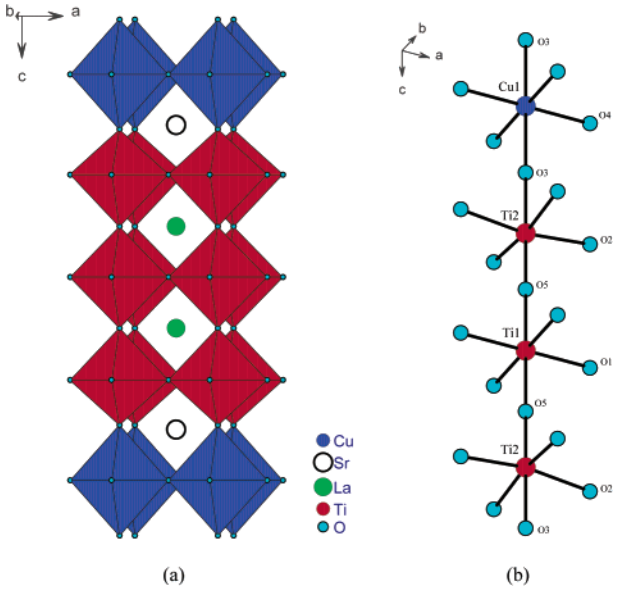

Figure 4. (a) Structure of $Sr_2La_2CuTi_3O_{12}$ (**I**). In (b) the oxygen coordinations around Ti and Cu are shown.

Table 1. Final Atomic Coordinates, Occupancies, and Atomic Displacement Parameters (B_{iso}) for $Sr_2La_2CuTi_3O_{12}$[a]

atom	Wyckoff posn	x	y	z	occ	B_{iso} (Å^2)
Cu1	1a	0	0	0	1	2.2(2)
Sr1	2h	0.5	0.5	0.1248(6)	0.53	2.5(1)
La1	2h	0.5	0.5	0.1248(6)	0.47	2.5(1)
Sr2	2h	0.5	0.5	0.3748(6)	0.47	2.5(1)
La2	2h	0.5	0.5	0.3748(6)	0.53	2.5(1)
Ti1	1b	0	0	0.5	1	0.79(7)
Ti2	2g	0	0	0.2603(8)	1	0.79(7)
O1	2e	0	0.5	0.5	1	3.4(2)
O2	4i	0	0.5	0.247(3)	1	3.4(2)
O3	2g	0	0	0.136(3)	1	3.4(2)
O4	2f	0	0.5	0	1	3.4(2)
O5	2g	0	0	0.375(5)	1	3.4(2)

[a] Lattice parameters $a = 3.9098(2)$ and $c = 15.794(1)$ Å. Space group: *P*4/*mmm*. $R_p = 4.28\%$, $R_{wp} = 5.85\%$, $R_{Bragg} = 4.86\%$, and $R_f = 4.56\%$.

Table 2. Selected Bond Lengths (Å) for $Sr_2La_2CuTi_3O_{12}$

Cu1−O3 (×2)	2.15(5)	Ti2−O2 (×4)	1.97(5)
Cu1−O4 (×4)	1.96(1)	Ti2−O3	1.96(5)
Ti1−O1 (×4)	1.96(1)	Ti2−O5	1.81(8)
Ti1−O5 (×2)	1.97(8)		

I drawn from the coordinates given in Table 1. The oxygen coordinations of Ti and Cu in the structure of **I** are shown in Figure 4b.

The structure of **I** consists of single ($CuO_{4/2}O_{2/2}$) perovskite-like sheets alternating with perovskite sheets of triple ($Ti_3O_{18/2}$) octahedra along the *c*-direction, the cubooctahedral sites being occupied by La/Sr. Refinement of occupancies (Table 1) clearly shows that there is no mixing of Ti/Cu in the structure, while there is a considerable La/Sr mixing; indeed, the 47/53 distribution of La/Sr in the structure suggests a near random distribution of La/Sr at the cubooctahedral sites. But, the ordering/nonmixing of Cu/Ti in the structure is particularly significant, revealing that distinct $CuO_{4/2}O_{2/2}$ sheets occur in the structure. Bond lengths of Ti(1)O_6 and Ti(2)O_6 octahedra (Table 2) are similar to those of $K_2La_2Ti_3O_{10}$.[10] Also the bond lengths of $CuO_{4/2}O_{2/2}$

(10) Toda, K.; Watanabe, J.; Sato, M. *Mater. Res. Bull.* **1996**, *31*, 1427−1435.

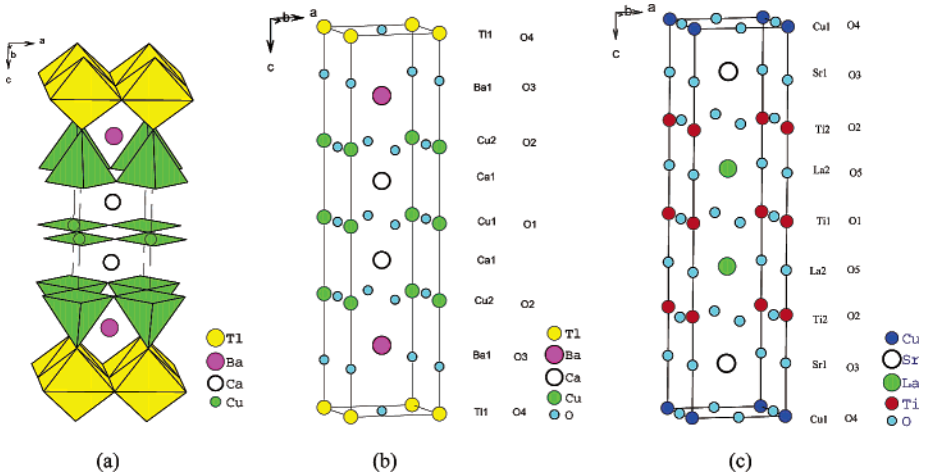

(a) (b) (c)

Figure 5. (a) Structure of $TlBa_2Ca_2Cu_3O_9$ (drawn from coordinates given in ref 12), (b) unit cell of $TlBa_2Ca_2Cu_3O_9$, and (c) unit cell of $Sr_2La_2CuTi_3O_{12}$.

octahedra are similar to those[11] of $La_2CuO_4/La_{1.85}Sr_{0.15}CuO_4$ and $Tl_2Ba_2CuO_6$.[11] The first-order Jahn−Teller distortion of CuO_6 octahedra and the second-order Jahn−Teller distortion of terminal $Ti(2)O_6$ octahedra in **I** are clearly retained from the parents ($Sr_2CuO_2Cl_2$ and $K_2La_2Ti_3O_{10}$). Accordingly, the metathetical reaction (eq 1) could be regarded as topochemical, despite the mixing of La/Sr.

The structure of the quadruple perovskite, $Sr_2La_2CuTi_3O_{12}$ (**I**), is related to those[12,13] of the superconducting $TlBa_2Ca_2Cu_3O_9$ and $Tl_{0.5}Pb_{0.5}Sr_2Ca_2Cu_3O_9$. The structure of $TlBa_2Ca_2Cu_3O_9$ is shown in Figure 5a. The unit cell dimensions of $Sr_2La_2CuTi_3O_{12}$ (Figure 5c) are closely similar to the unit cell dimensions of $TlBa_2Ca_2Cu_3O_9$ (Figure 5b). The crystallographic relationship between $Sr_2La_2CuTi_3O_{12}$ and $TlBa_2Ca_2Cu_3O_9$ is as follows:

$Sr_2La_2CuTi_3O_{12}$		$TlBa_2Ca_2Cu_3O_9$	
space group	*P4/mmm*	space group	*P4/mmm*
lattice params (Å)	$a = 3.9098(2)$, $c = 15.794(1)$	lattice params (Å)	$a = 3.853(1)$, $c = 15.913(4)$
atomic posn		atomic posn	
1a	Cu	1a	Tl
2h	Sr1/La1	2h	Ba
2h	La2/Sr2	2h	Ca
1b	Ti1	1b	Cu1
2g	Ti2	2g	Cu2
2e	O1	2e	O1
4i	O2	4i	O2
2g	O3	2g	O3
2f	O4 (0 0.5 0)	1c	O4 (0.5 0.5 0)
2g	O5 (0 0 0.375)		

We see clearly that the Cu atoms in $TlBa_2Ca_2CuO_9$ are replaced by Ti in $Sr_2La_2CuTi_3O_{12}$; instead of rock salt like TlO layers in $TlBa_2Ca_2Cu_3O_9$, we have CuO_2 sheets in $Sr_2La_2CuTi_3O_{12}$ with additional oxygen (O5) at the 2g site. Also, the face-centered oxygen (O4) at the 1c site in $TlBa_2Ca_2Cu_3O_9$ is shifted to edge center (2f site) in $Sr_2La_2CuTi_3O_{12}$.

Table 3. Final Atomic Coordinates, Occupancies, and Atomic Displacement Parameters (B_{iso}) for $Ca_2La_2CuTi_3O_{12}$[a]

atom	Wyckoff posn	x	y	z	occ	B_{iso} (Å^2)
Cu	1a	0	0	0	1	2.6(7)
Ca1	2h	0.5	0.5	0.1269(8)	0.52	3.3(1)
La1	2h	0.5	0.5	0.1269(8)	0.48	3.3(1)
Ca2	2h	0.5	0.5	0.3718(9)	0.48	3.3(1)
La2	2h	0.5	0.5	0.3718(9)	0.52	3.3(1)
Ti1	1b	0	0	0.5	1	1.3(3)
Ti2	2g	0	0	0.255(2)	1	1.3(3)
O1	2e	0	0.5	0.5	1	5.7(2)
O2	4i	0	0.5	0.248(4)	1	5.7(2)
O3	2g	0	0	0.130(4)	1	5.7(2)
O4	2f	0	0.5	0	1	5.7(2)
O5	2g	0	0	0.381(4)	1	5.7(2)

[a] Lattice parameters $a = 3.8729(5)$ and $c = 15.689(2)$ Å. Space group: *P4/mmm*. $R_p = 5.35\%$, $R_{wp} = 6.92\%$, $R_{Bragg} = 8.70\%$, and $R_f = 7.96\%$.

$Ba_2La_2Cu_2Sn_2O_{11}$ and the related titanium analogues[14] are also regarded as quadruple perovskites, but here the double Sn_2O_6 octahedral sheets alternate with double square-pyramidal Cu_2O_5 sheets.

Electron diffraction (ED) patterns of **I** (Figure 6) are consistent with the structure (Figure 4) obtained from the XRD data. While the ~3.9 × 3.9 Å ($a_p \times a_p$) cell in the $a-b$ plane is clearly seen in the ED pattern (Figure 6a), the quadruple c parameter is not very clear (Figure 6b). Instead we see a streaking in the c^* direction which most likely arises from poor crytallinity and lower temperature synthesis.

Having succeeded in the synthesis of novel quadruple perovskite **I**, we have extended our metathesis route to synthesize $Ca_2La_2CuTi_3O_{12}$ (**II**). The powder XRD pattern (Figure 7) of the washed product obtained from the reaction between $K_2La_2Ti_3O_{10}$ and $Ca_2CuO_2Cl_2$ at 750 °C for 24 h in air with one intermediate grinding reveals the formation of **II**. The powder XRD pattern of **II** could be indexed on a tetragonal cell with the lattice parameters $a = 3.870(1)$ and $c = 15.645(4)$ Å, which are similar to the lattice parameters of **I** ($a = 3.9098(2)$ and $c = 15.794(1)$ Å). We have refined the structure of **II** from powder XRD data (Figure 8; Table 3) using the structure of **I** as the model. The satisfactory refinement suggests that **II** is most likely isostructural with **I**.

(11) (a) Longo J. M.; Raccah, P. M. *J. Solid State Chem.* **1973**, *6*, 526−531. (b) Yvon K.; Francois, M. *Z. Phys. B: Condens. Matter* **1989**, *76*, 413−444.
(12) Subramanian, M. A.; Parise, J. B.; Calabrese, J. C.; Torardi, C. C.; Gopalakrishnan, J.; Sleight, A. W. *J. Solid State Chem.* **1988**, *77*, 192−195.
(13) Subramanian, M. A.; Torardi, C. C.; Gopalakrishnan, J.; Gai, P. L.; Calabrese, J. C.; Askew, T. R.; Flippen, R. B.; Sleight, A. W. *Science* **1988**, *242*, 249−252.
(14) (a) Anderson, M. T.; Poeppelmeier, K. R.; Zhang, J.-P.; Fan, H.-J.; Marks, L. D. *Chem. Mater.* **1992**, *4*, 1305−1313. (b) Gómez-Romero, P.; Palacin, M. R.; Rodríguez-Carvajal, J. *Chem. Mater.* **1994**, *6*, 2118−2122.

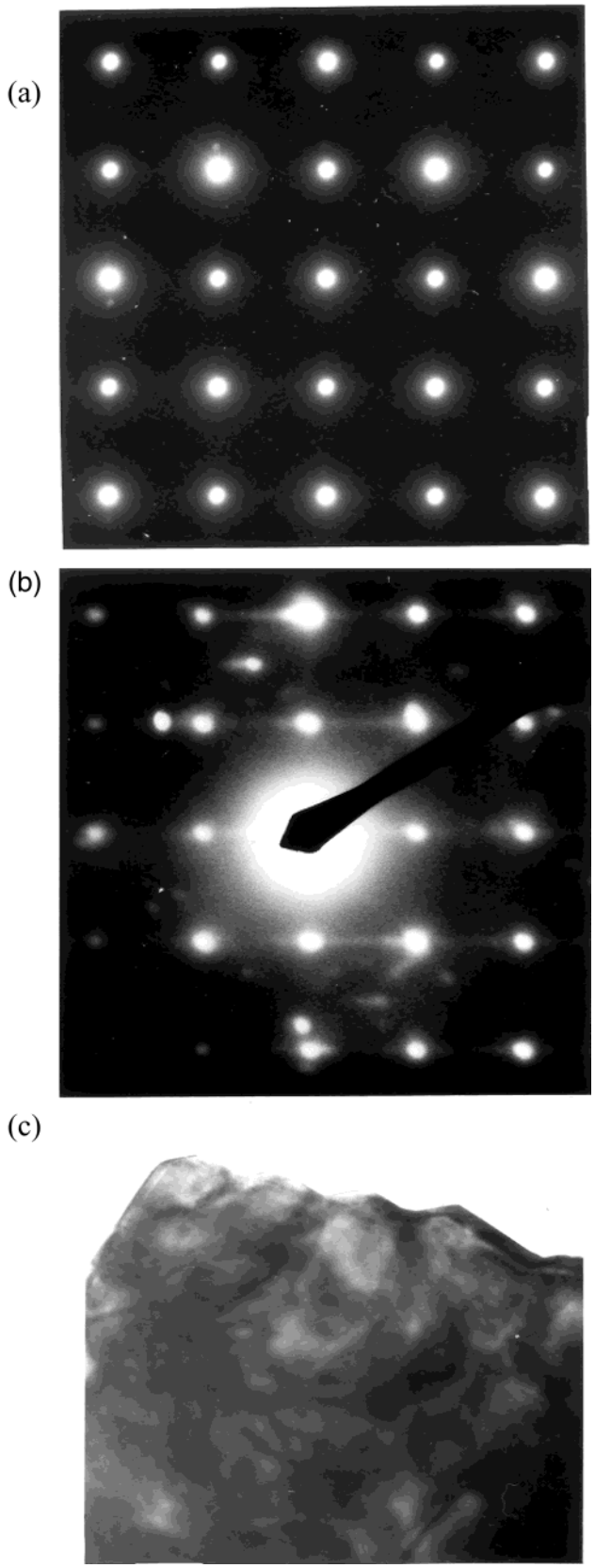

Figure 6. Electron diffraction patterns of **I** recorded (a) along the (001) beam direction and (b) along the (100) beam direction. The bright field image of the particle is shown in (c).

Interestingly, the reaction of $K_2La_2Ti_3O_{10}$ with $Ca_2CuO_2Cl_2$ at 650 °C follows a different pathway yielding a new layered perovskite titanate:

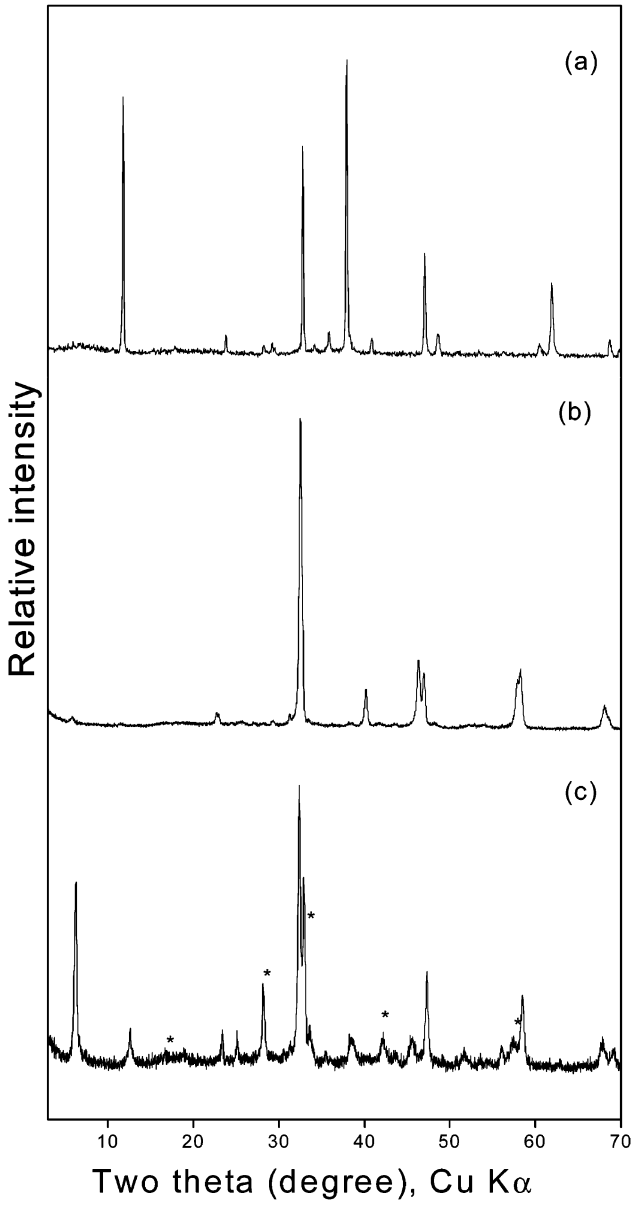

Figure 7. Powder XRD patterns of (a) $Ca_2CuO_2Cl_2$, (b) $Ca_2La_2CuTi_3O_{12}$ (**II**), and (c) $CaLa_2Ti_3O_{10} + CaCuO_2$. Reflections due to $CaCuO_2$ are marked by asterisks in (c).

$$K_2La_2Ti_3O_{10} + Ca_2CuO_2Cl_2 \rightarrow CaLa_2Ti_3O_{10} + CaCuO_2 + 2KCl \quad (2)$$

Powder XRD pattern of the product (Figure 7c) after washing to remove KCl shows clearly the presence of two phases $CaLa_2Ti_3O_{10}$ and $CaCuO_2$. The XRD pattern of $CaLa_2Ti_3O_{10}$ is similar to the pattern of $CoLa_2Ti_3O_{10}$[15] and is indexable on a tetragonal system (Table 4) with $a = 7.680(3)$ and $c = 13.95(1)$ Å. The ED patterns (Figure 9) are also consistent with tetragonal layered structure for $CaLa_2Ti_3O_{10}$.

Both **I** and **II** transform at higher temperatures to 3D perovskites. **I** on heating at 1100 °C for 24 h transforms to a cation disordered simple cubic perovskite, $Sr_2La_2CuTi_3O_{12}$ (**Ia**) (Figure 10) with lattice parameter $a = 3.915(1)$ Å. ED pattern (Figure 11a) showing $a_p \sim 3.9$ Å is also consistent

(15) Hyeon, K.-A.; Byeon, S.-H. *Chem. Mater.* **1999**, *11*, 1, 352−357.

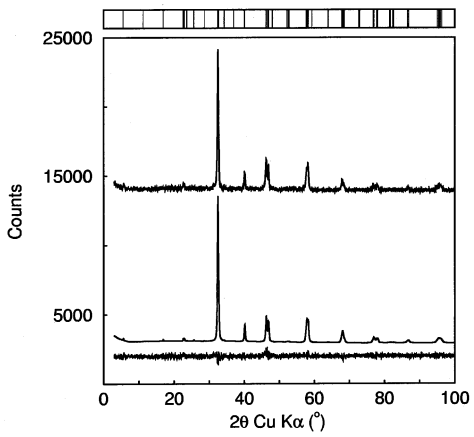

Figure 8. Observed (top), Rietveld refined (middle), and difference (bottom) XRD profiles of $Ca_2La_2CuTi_3O_{12}$. Vertical lines on the top panel above the figure indicate the expected Bragg reflections in the space group *P*4/*mmm*.

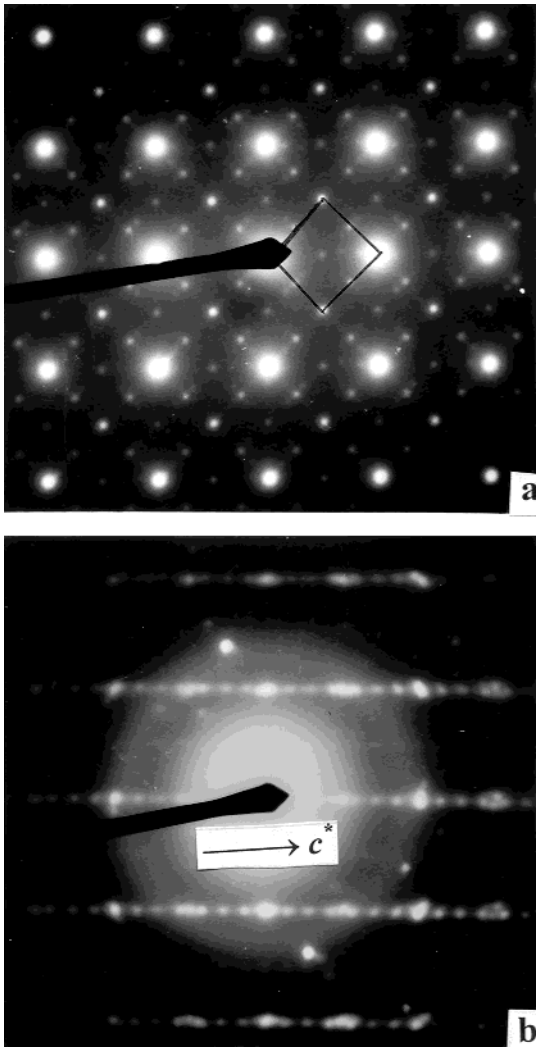

Figure 9. ED patterns for (a) $CaLa_2Ti_3O_{10}$ recorded with the beam direction along (001) showing the $2a_p \times 2a_p$ cell and (b) $CaLa_2Ti_3O_{10}$ recorded with the beam direction along (010) showing ~14 Å periodicity in the *c**-direction.

with the powder XRD data. Interestingly, the powder XRD pattern (Figure 10) of the product (**IIa**) obtained on heating **II** at 1000 °C for 48 h with an intermediate grinding shows

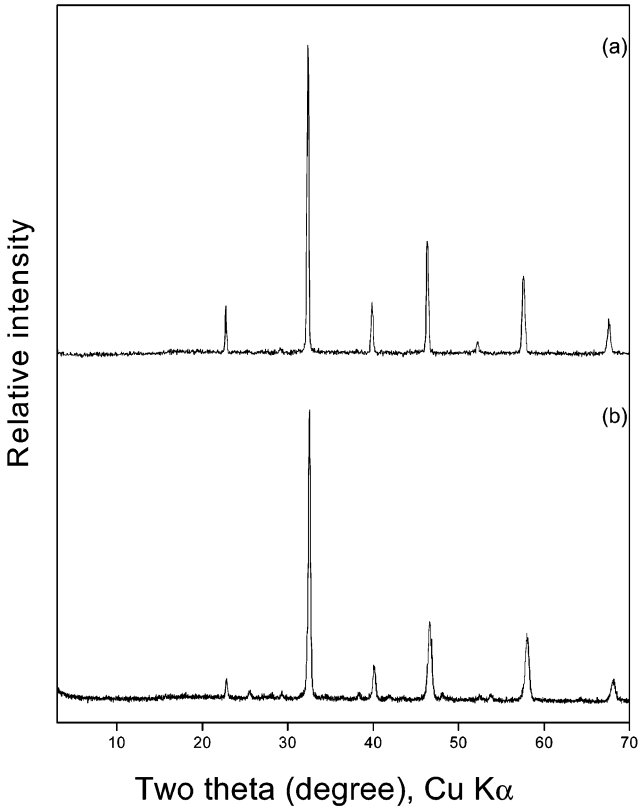

Figure 10. Powder XRD patterns of (a) $Sr_2La_2CuTi_3O_{12}$ (**Ia**) and (b) $Ca_2La_2CuTi_3O_{12}$ (**IIa**) obtained by heating **I** and **II** at high temperature (1000−1100 °C).

Table 4. Powder XRD Data for $CaLa_2Ti_3O_{10}$

h	k	l	d_{obsd} (Å)	d_{calcd}[a] (Å)	I_{obsd}
0	0	1	14.12	13.95	66
0	0	2	7.02	6.97	14
2	0	0	3.81	3.84	13
1	1	3	3.543	3.532	12
1	0	4	3.167	3.175	26
2	1	3	2.763	2.763	100
2	2	0	2.716	2.715	63
2	2	1	2.670	2.665	15
2	2	2	2.530	2.530	6
2	2	3	2.341	2.345	11
2	2	4	2.143	2.142	10
3	1	4	1.993	1.993	11
4	0	0	1.921	1.920	33
2	2	6	1.766	1.766	6
4	1	4	1.642	1.643	7
2	2	7	1.606	1.606	11
4	0	5	1.580	1.581	25
5	1	4	1.383	1.383	11
4	4	0	1.358	1.358	8

[a] $a = 7.680(3)$ and $c = 13.95(1)$ Å.

a striking similarity to that of La_2CuMnO_6[16] and is indexable on a cubic double perovskite cell (Table 5). SEM of **IIa** shows a single phase, and the EDX spectrum corresponds to Ca:La:Cu:Ti ratio as 2:2:1:3. The corresponding ED pattern of **IIa** (Figure 11b) is also consistent with a perovskite cell having $a_p \sim 7.8$ Å. The high-temperature phase **IIa** is however not an ordered double perovskite[17] of $A_2BB'O_6$ type. The occurrence of mixed *hkl* reflections, 300, 210, 320, 410,

(16) Anderson, M. T.; Greenwood, K. B.; Taylor, G. A.; Poeppelmeier, K. R. *Prog. Solid State Chem.* **1993**, *22*, 197−233.

Table 5. Powder XRD Data for $Ca_2La_2CuTi_3O_{12}$ (**IIa**)

h	*k*	*l*	d_{obsd} (Å)	d_{calcd}[a] (Å)	I_{obs}
2	0	0	3.892	3.890	7
2	1	0	3.476	3.479	3
2	2	0	2.750	2.750	100
3	0	0	2.598	2.593	1
3	1	1	2.346	2.346	2
2	2	2	2.246	2.246	11
3	2	0	2.157	2.158	1
4	0	0	1.945	1.945	26
4	1	0	1.887	1.887	3
4	2	0	1.740	1.740	2
4	2	1	1.698	1.698	1
4	2	2	1.588	1.588	23
4	4	0	1.375	1.375	7
6	2	0	1.230	1.230	6
6	3	0	1.160	1.160	1
4	4	4	1.123	1.123	2
6	4	0	1.079	1.079	1
6	4	2	1.040	1.040	7

[a] $a = 7.780(1)$ Å.

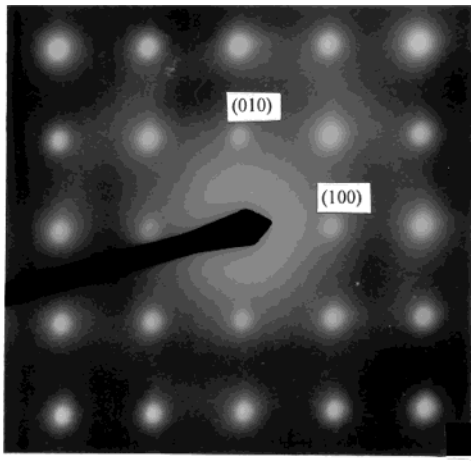

(a)

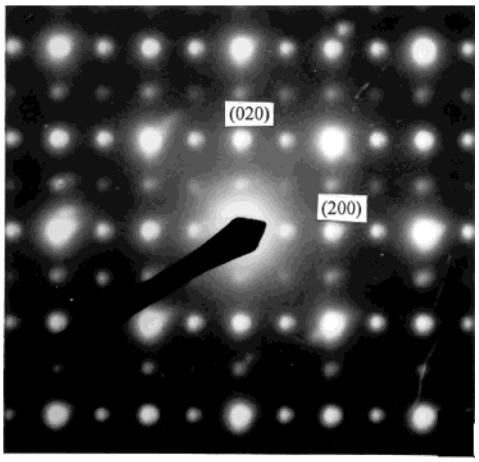

(b)

Figure 11. ED patterns for (a) $Sr_2La_2CuTi_3O_{12}$ (**Ia**) showing $a = a_p$ ($a_p \sim 3.9$ Å) and (b) $Ca_2La_2CuTi_3O_{12}$ (**IIa**) showing $a \sim 2a_p$ ($a_p \sim 3.9$ Å).

421, and 630 (Table 5), rules out this possibility. We believe that the structures of the high-temperature form of $Ca_2La_2CuTi_3O_{12}$ (**IIa**) and La_2CuMnO_6 are quite related but not the same as a regular double perovskite with *Fm*3*m* symmetry, albeit the unit cells being cubic with $a \approx 7.78$ Å. The lattice parameters of the new quadruple and 3D perovskites synthesized are summarized in Table 6.

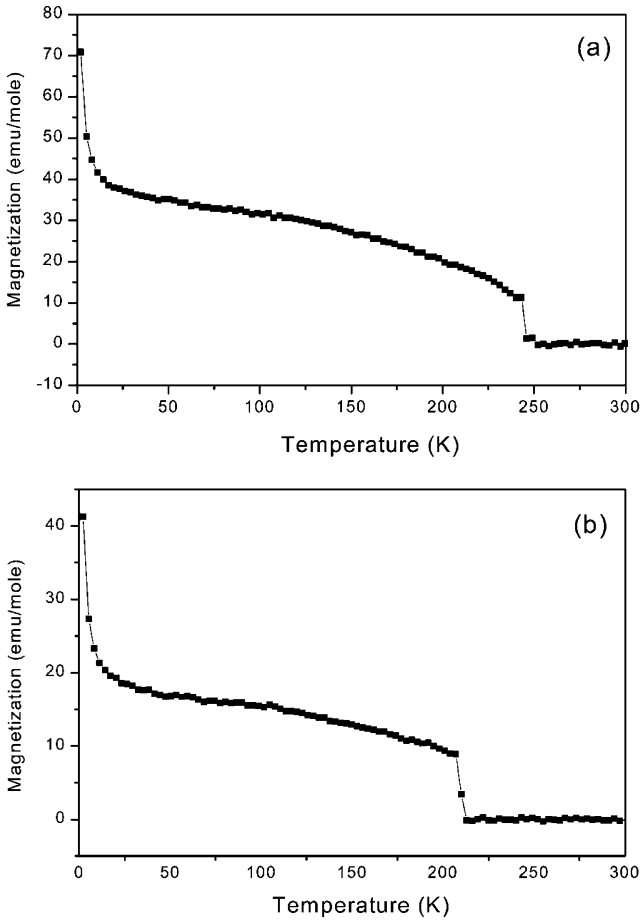

Figure 12. Magnetization vs temperature plots for (a) $Sr_2La_2CuTi_3O_{12}$ (**I**) and (b) $Ca_2La_2CuTi_3O_{12}$ (**II**).

Table 6. Summary of the New Perovskite-Related Oxides Synthesized by Metathesis Reactions between $K_2La_2Ti_3O_{10}$ and $A_2CuO_2Cl_2$ (A = Sr, Ca)

compd	structure	lattice params (Å)
$Sr_2La_2CuTi_3O_{12}$ (**I**)	quadruple perovskite	tetragonal: $a = 3.9098(2)$; $c = 15.794(1)$
$Ca_2La_2CuTi_3O_{12}$ (**II**)	quadruple perovskite	tetragonal: $a = 3.8729(5)$; $c = 15.689(2)$
$Sr_2La_2CuTi_3O_{12}$ (**Ia**)	3D perovskite	cubic: $a = 3.915(1)$
$Ca_2La_2CuTi_3O_{12}$ (**IIa**)	3D perovskite	cubic: $a = 7.780(1)$
$CaLa_2Ti_3O_{10}$	layered perovskite	tetragonal: $a = 7.680(3)$; $c = 13.95(1)$

Figure 12 shows the magnetization of **I** and **II** measured at an applied field of 500 Oe. The magnetization is small, and there is a reproducible jump between 200 and 250 K, which could be due to onset of magnetic ordering. Magnetization recorded at higher fields is similar aside from a small increase, apparently due to a small amount of Curie impurities or defects, which can also be seen from the "Curie tail" below ~10 K (Figure 12). The net moments are 0.0065 μ_B for **I** and 0.0033 μ_B for **II**, which were determined by plotting the moment versus field at low temperatures and extrapolating to zero field. The ordering temperatures are similar to those of La_2CuO_4[18] and the other K_2NiF_4-like cuprates such

(17) Mitchell, R. H. *Perovskites: Modern and Ancient*; Almaz Press: Thunder Bay, Canada, 2002; pp 79−82.

as $Sr_2CuO_2Cl_2$[19] containing strong antiferromagnetically coupled CuO_2 sheets. The jump in the magnetization around 250 K could arise from a "canting" of spins due to Dzyaloshinsky−Moriya type interaction.[20] This interaction is present in orthorhombic La_2CuO_4 but not in tetragonal $Sr_2CuO_2Cl_2$.[19] **I** and **II** are assigned tetragonal structures on the basis of powder XRD data, but a small distortion to orthorhombic symmetry could occur at low temperatures. Further structural investigations are needed to clarify these aspects.

Dc electrical resistivity measurements show that both **I** and **II** are semiconductors (ρ at 300 K $\sim 10^4-10^6$ Ω cm) with activation energies of 0.29 and 0.18 eV, respectively. The high resistivity could in part be due to poor sinterability of the materials.

Conclusion

We have synthesized new quadruple perovskite oxides, $A_2La_2CuTi_3O_{12}$ (A = Sr, Ca), by a novel metathesis reaction between the 2D-layered perovskites, $K_2La_2Ti_3O_{10}$ and $A_2CuO_2Cl_2$ (A = Sr, Ca). We have determined the crystal structures of the quadruple perovskites, $Sr_2La_2CuTi_3O_{12}$ and $Ca_2La_2CuTi_3O_{12}$, by Rietveld refinement of the powder XRD data. To our knowledge, $A_2La_2CuTi_3O_{12}$ described here are the first examples of true quadruple perovskites without oxygen vacancy and with a distinct ordering of Cu and Ti atoms in the octahedral sites. Considering that the new quadruple perovskites contain CuO_2 sheets similar to those found in superconducting cuprates, we believe the quadruple perovskites described here deserve further attention for possible realization of superconductivity.

Acknowledgment. We thank the Department of Science and Technology, Government of India, New Delhi, for support of this research work. S.E.L. and K.V.R. acknowledge the support of the New Jersey Commission on Higher Education.

Supporting Information Available: Tables S1 and S2, giving powder XRD data for $Sr_2La_2CuTi_3O_{12}$ (**I**) and $Ca_2La_2CuTi_3O_{12}$ (**II**), respectively. This material is available free of charge via the Internet at http://pubs.acs.org.

IC035358L

(18) For example, see: (a) Ting, S. T.; Pernambuco-Wise, P.; Crow, J. E.; Manousakis, E. *Phys. Rev. B* **1992**, *46*, 11772−11778. (b) Thio, T.; Aharony, A. *Phys. Rev. Lett.* **1994**, *73*, 894−897.

(19) Vaknin, D.; Sinha, S. K.; Stassis, C.; Millner, L. L.; Johnson, D. C. *Phys. Rev B* **1990**, *41*, 1926−1933.

(20) (a) Dzyaloshinsky, I. *J. Phys. Chem. Solids* **1958**, *4*, 241−255. (b) Moriya, T. *Phys. Rev.* **1960**, *120*, 91−98.